

**Identification of substitutional Li in *n*-type ZnO and its role as an acceptor**K. M. Johansen,<sup>1</sup> A. Zubiaga,<sup>2</sup> I. Makkonen,<sup>3</sup> F. Tuomisto,<sup>2</sup> P. T. Neuvonen,<sup>1</sup> K. E. Knutsen,<sup>1</sup> E. V. Monakhov,<sup>1</sup>  
A. Yu. Kuznetsov,<sup>1</sup> and B. G. Svensson<sup>1</sup><sup>1</sup>*University of Oslo, Centre for Materials Science and Nanotechnology, 0318 Oslo, Norway*<sup>2</sup>*Department of Applied Physics, Aalto University, P.O. Box 11100, 00076 Aalto, Espoo, Finland*<sup>3</sup>*Helsinki Institute of Physics and Department of Applied Physics, Aalto University, P.O. Box 14100, 00076 Aalto, Espoo, Finland*

(Received 7 December 2010; revised manuscript received 25 February 2011; published 27 June 2011)

Monocrystalline *n*-type zinc oxide (ZnO) samples prepared by different techniques and containing various amounts of lithium (Li) have been studied by positron annihilation spectroscopy (PAS) and secondary ion mass spectrometry. A distinct PAS signature of negatively charged Li atoms occupying a Zn-site ( $\text{Li}_{\text{Zn}}^-$ ), so-called substitutional Li, is identified and thus enables a quantitative determination of the content of  $\text{Li}_{\text{Zn}}$ . In hydrothermally grown samples with a total Li concentration of  $\sim 2 \times 10^{17} \text{ cm}^{-3}$ ,  $\text{Li}_{\text{Zn}}$  is found to prevail strongly, with only minor influence, by other possible configurations of Li. Also in melt grown samples doped with Li to a total concentration as high as  $1.5 \times 10^{19} \text{ cm}^{-3}$ , a considerable fraction of the Li atoms (at least 20%) is shown to reside on the Zn-site, but despite the corresponding absolute acceptor concentration of  $\geq (2-3) \times 10^{18} \text{ cm}^{-3}$ , the samples did not exhibit any detectable *p*-type conductivity. The presence of  $\text{Li}_{\text{Zn}}$  is demonstrated to account for the systematic difference in positron lifetime of 10–15 ps between Li-rich and Li-lean ZnO materials as found in the literature, but further work is needed to fully elucidate the role of residual hydrogen impurities and intrinsic open volume defects.

DOI: [10.1103/PhysRevB.83.245208](https://doi.org/10.1103/PhysRevB.83.245208)

PACS number(s): 81.05.Dz, 71.15.Mb, 71.55.Gs, 78.70.Bj

**I. INTRODUCTION**

For a long time, the fundamental challenge of accomplishing stable *p*-type ZnO has hampered the realization of optoelectronic devices such as white light emitting diodes and UV-laser diodes based on ZnO. One of the candidates for *p*-type doping of ZnO has been Li substituting on the Zn-site ( $\text{Li}_{\text{Zn}}$ ) despite results indicating not a very shallow acceptor state in the bandgap.<sup>1-3</sup> However, one ultimate challenge is the amphoteric nature of Li where Li on an interstitial site ( $\text{Li}_i$ ) acts as a donor, leading to self-compensation. The fraction between donor and acceptor states is dependent on the electrochemical potential of the material.<sup>4-6</sup> Further, based on density functional theory, Wardle *et al.*<sup>5</sup> have predicted the existence of a neutral  $\text{Li}_{\text{Zn}}\text{-Li}_i$  complex. Because of the low formation energy of this complex, as compared to the sum of that for isolated  $\text{Li}_{\text{Zn}}$  and  $\text{Li}_i$ , they suggested that the complex may dominate the behavior of Li in ZnO. Moreover,  $\text{Li}_{\text{Zn}}$  can also be passivated by H and form the  $\text{OH-Li}_{\text{Zn}}$  complex, which occurs as a neutral defect.<sup>5,7-10</sup>

However, in *n*-type hydrothermally grown (HT) ZnO samples with unintentional concentrations of Li in the  $(1-5) \times 10^{17} \text{ cm}^{-3}$  range, it is shown experimentally that decreasing the concentration of Li leads to an increase in the conductivity, consistent with Li mainly being in the acceptor configuration,  $\text{Li}_{\text{Zn}}^-$ .<sup>11,12</sup> Electron paramagnetic resonance (EPR) measurements of Li-rich ZnO have also revealed that a measurable fraction of the Li atoms reside on the Zn-site.<sup>13</sup> In a few studies, Li has also been observed to contribute to *p*-type doping in ZnO thin polycrystalline films grown by dc reactive magnetron sputtering.<sup>14,15</sup> Recently, an acceptor state was observed by photoluminescence in Li-doped<sup>16</sup> and H-doped<sup>2</sup> samples in the temperature range between 400–600 °C and 500–550 °C, respectively, possibly originating from a  $\text{Li}_{\text{Zn}}\text{-H-Li}_{\text{Zn}}$  complex.<sup>2,16</sup>

Positron annihilation spectroscopy (PAS) is an invaluable tool in the search for neutral and negatively charged open volume defects in many semiconductors, including ZnO.<sup>17-19</sup> In 1992, de la Cruz *et al.*<sup>20</sup> measured the average positron lifetime ( $\tau_{\text{ave}}$ ) in flux grown ZnO samples and observed single component lifetimes of  $180 \pm 3$  and  $169 \pm 2$  ps in as-grown and thermochemically reduced samples, respectively. The 169 ps lifetime was attributed to the bulk positron lifetime ( $\tau_B$ ), while the defect responsible for the 180 ps lifetime remained unidentified. More recently, Tuomisto *et al.*<sup>18,21</sup> found the same  $\tau_{\text{ave}}$  of 170 ps in samples prepared by the seeded vapor phase technique (VP-ZnO), supporting the assignment of the  $169 \pm 2$  ps lifetime being the  $\tau_B$  in ZnO. A bulk positron lifetime of  $171 \pm 1$  ps in VP-ZnO samples (supplied by Eagle-Picher) was also observed by Chen *et al.*<sup>22</sup> In as-grown HT-ZnO (SPC-Goodwill), on the other hand, Chen *et al.* found a single component positron lifetime ranging from  $182.2 \pm 0.7$  to  $198 \pm 1$  ps depending on the specific wafer measured.<sup>22-24</sup> They speculated that this variation was related to annihilation of positrons at other sites than those in a perfect crystal, such as impurities, small angle grain boundaries, or some other unknown imperfections, homogeneously distributed in the material. In hydrothermally grown material originating from several different suppliers studied by Brauer *et al.*,<sup>25</sup> the  $\tau_{\text{ave}}$  is found to be in the range of 180–182 ps, while in melt grown samples, the  $\tau_{\text{ave}}$  is in the range of 165–167 ps. Finally, a similar difference of  $\sim 10$  ps between HT samples (CrysTec) and VP samples (Eagle-Picher) was also reported by Brunner *et al.*,<sup>17</sup> despite somewhat lower absolute values than those in Refs. 18 and 20–25. Further, conducting PAS Doppler broadening experiments, Børseth *et al.*<sup>26</sup> observed a deviation of the annihilation parameter values for N-implanted HT samples as compared to those for samples grown by the VP technique. Such a deviation was not observed using ZnO thin

films grown by molecular-beam epitaxy<sup>27</sup> or by metalorganic chemical vapor deposition.<sup>28</sup>

Brauer *et al.*<sup>25</sup> have proposed that the discrepancy in the single component positron lifetime of single crystalline ZnO materials grown by different techniques is due to  $V_{Zn}-H_n$  complexes; in Ref. 25, samples with H concentration as high as 0.3 at.%, measured by nuclear reaction analysis (NRA), were studied. Such a high H concentration is, as mentioned by the authors themselves, not consistent with the findings of Ohashi *et al.*<sup>29</sup> and Nickel and Brendel.<sup>30</sup> Furthermore, recent results by Vines *et al.*<sup>12</sup> reveal H concentrations below  $5 \times 10^{17} \text{ cm}^{-3}$  in hydrothermally grown ZnO (SPC-Goodwill). H-concentrations in the at. % range are also in strong contrast to the H solubility limits estimated by Thomas and Lander.<sup>31</sup> The origin of this discrepancy in the H-concentration as measured by NRA and other methods such as secondary ion mass spectrometry (SIMS) and effusion measurements is not known and needs further attention.

In this work, PAS, SIMS, and four-point probe measurements have been employed to study n-type bulk ZnO samples prepared by different techniques and with different concentrations of Li. The PAS signature of negatively charged substitutional Li,  $Li_{Zn}$  is identified; a clear correlation between the increased single component positron lifetime and the  $Li_{Zn}$  concentration is revealed together with distinct signatures deduced from the Doppler broadening spectra. These conclusions are supported by modeling of the PAS parameters using electron structure calculations. Through correlation between the PAS and SIMS data, the fraction of Li in substitutional configuration is quantitatively determined and its importance as an acceptor center in the different samples is discussed.

## II. METHODOLOGY

Four n-type HT-ZnO wafers (labeled HT 1–4) supplied by SPC-Goodwill were used in this study. A concentration of  $2 \times 10^{17} \text{ Li/cm}^3$  was found in the as-grown material (wafer HT-1), as measured by SIMS, using a Cameca IMS7f microanalyzer. Samples HT-2, HT-3, and HT-4 were heat treated in air at 1500 °C for 1 h in order to reduce the Li content to the  $10^{15} \text{ cm}^{-3}$  range and then mechanically polished at the O-face to restore the surface smoothness.<sup>11</sup> The sample HT-2 was subsequently heat treated further at 1100 °C for 1 h to minimize the influence of polishing defects in the near surface region on the slow positron beam measurements.<sup>32</sup> Two melt grown (MG) samples (labeled MG-1 and MG-2) with a resistivity of 1–2  $\Omega \text{ cm}$  were purchased from Cermet Inc. and contained a Li concentration of  $\sim 10^{15} \text{ cm}^{-3}$  in the as-grown state. Li was intentionally introduced into sample MG-2 by annealing at 600 °C for 1 h in a closed quartz ampoule containing a mixture of 10%  $Li_2O$  and 90% ZnO powders, resulting in a highly resistive material (the resistivity exceeded 10 k $\Omega \text{ cm}$  as determined by four-point probe measurements).

The positron lifetimes were measured using a conventional fast-fast coincidence spectrometer with a Gaussian time resolution with full width at half maximum of 250 ps (Ref. 33). Two identical sample pieces were sandwiched with a 20  $\mu\text{Ci}$  positron source ( $^{22}\text{Na}$  deposited on a 1.5  $\mu\text{m}$  Al foil). Typically  $2 \times 10^6$  annihilation events were collected in each positron lifetime spectrum. The lifetime spectra

were analyzed as the sum of exponential decay components convoluted with the resolution function of the spectrometer, after subtracting material-specific values for the constant background and annihilation in the source material and as positronium (215 ps, 2.0%; 400 ps, 3.4%; 1500 ps, 0.08%). For the Doppler broadening experiments, the samples were studied with monoenergetic positrons implanted into the O-face at room temperature. The implantation energy of the positrons was varied in the range of 0.5–38 keV, giving a mean positron implantation depth of 0.05–2.4  $\mu\text{m}$ . The Doppler broadening of the annihilation radiation was detected with two Ge detectors with an energy resolution of 1.24 keV at 511 keV. The data were analyzed using the conventional *S*- and *W*-parameters, defined as the fractions of counts in the central *S*,  $|E - 511 \text{ keV}| \leq 0.8 \text{ keV}$  (corresponding to electron-positron pair momentum of 0.4 a.u.), and the wing *W*,  $2.9 \text{ keV} \leq |E - 511 \text{ keV}| \leq 7.4 \text{ keV}$  (1.6–4.0 a.u.), parts of the recorded photon spectrum. In addition, coincidence Doppler broadening measurements were conducted at a positron implantation energy of 30 keV (i.e., probing depth of a few micrometers below the surface), using two Ge detectors in coincidence with a peak-to-background ratio of about  $2 \times 10^6$ .

The so-called ratio curves for positron annihilation at different kinds of defect structures relative to that in a perfect crystal have been calculated. The technical details of the formalism used can be found in Ref. 34. To summarize, the positron annihilation parameters are modeled using electronic structure calculations; the valence electron densities are obtained self-consistently via the local-density approximation (LDA), employing the projector augmented-wave (PAW) method<sup>35</sup> and the plane-wave code VASP.<sup>36,37</sup> The positron states and annihilation characteristics are determined using the LDA (Ref. 38) and the state-dependent scheme<sup>39</sup> for the momentum densities of annihilating electron-positron pairs. For the most part, orthorhombic 96-atom cells are used, but the convergence of the positron state and lifetime have also been confirmed with 768-atom supercells. Defect structures are relaxed taking into account the forces exerted on the ions by the localized positron. The Doppler spectra are computed using the all-electron valence wave functions of the PAW method<sup>40</sup> and atomic orbitals for the core electrons. The spectra are then convoluted with the resolution of the Doppler measurements. The above approach is well-established and has been proven successful in various PAS studies (see, for instance, Refs. 41–43).

## III. RESULTS AND DISCUSSION

Figure 1 shows the Li-concentration as a function of depth in the studied samples. The as-grown HT-1 sample and the Li-reduced HT-2 sample contain  $2 \times 10^{17} \text{ Li/cm}^3$  and  $3 \times 10^{15} \text{ Li/cm}^3$ , respectively. It is important to note that the Li concentration is uniform in the samples up to a depth of at least 2–3  $\mu\text{m}$ . The as-grown MG-1 sample and the Li-enriched MG-2 sample contain  $1 \times 10^{15}$  and  $1.5 \times 10^{19} \text{ Li/cm}^3$ , respectively, and except for the near surface region ( $\leq 0.2 \mu\text{m}$ ), the profiles remain constant.

The average positron lifetime ( $\tau_{\text{ave}}$ ) in the sample HT-1 was found to be 187 ps at room temperature (RT), in good agreement with previous studies of HT ZnO in the as-grown

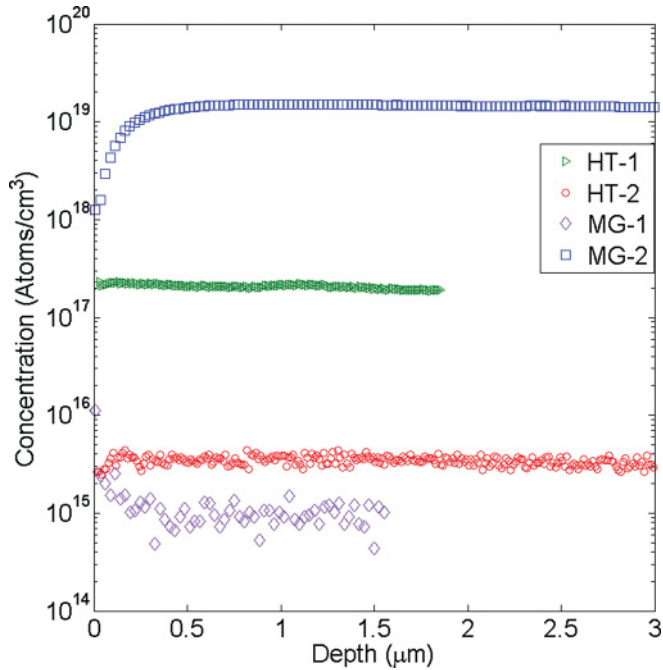


FIG. 1. (Color online) Li concentration versus depth profiles for samples HT-1, HT-2, MG-1, and MG-2 as measured by SIMS.

state, where values in the range of 180–190 ps have been reported.<sup>22–24</sup> The  $\tau_{\text{ave}}$  measured for samples HT-3 and HT-4 before and after the removal of Li, reveal a decrease of 6 ps from 184 to 178 ps and from 185 to 179 ps, respectively. The  $\tau_{\text{ave}}$  in the MG ZnO samples at RT was found to be 170 ps, as in the reference VP sample, and in good agreement with previous observations of the positron lifetime in “defect free” ZnO crystals (bulk lifetime,  $\tau_B$ ).<sup>21</sup> However, after introducing Li into the sample MG-2,  $\tau_{\text{ave}}$  increased by 10 ps to 180 ps. From this, we conclude that the longer  $\tau_{\text{ave}}$  (in the range of 180–190 ps) observed in the HT and Li-indiffused MG samples is related to the presence of Li. This is also consistent with the systematic positron lifetime difference of 10–15 ps between Li-rich (e.g., HT ZnO) and Li-lean ZnO, where a clear vacancy-related signal is not separable in the experimental lifetime spectra.<sup>17–22,24,44</sup> To illustrate the difference between samples with a low  $V_{\text{Zn}}$ -concentration and a high Li content, Fig. 2 shows the positron lifetime spectra for the VP reference sample, HT (or Li-indiffused MG) ZnO, and an electron irradiated VP sample<sup>27</sup> having similar  $\tau_{\text{ave}}$  as the as-grown HT samples. In irradiated samples, the longer  $\tau_{\text{ave}}$  (compared to the VP ZnO reference) is due to a longer and clearly resolved lifetime component emerging after 0.7 ns, while in the HT sample, the lifetime spectrum seems to consist of only a single component which is slightly longer than that in the VP reference sample. In the electron irradiated sample, the  $\tau_2 = 230 \pm 10$  ps component is caused by  $V_{\text{Zn}}$  while a Li-related defect with less open volume and a significant concentration [at least in the  $(2-3) \times 10^{17} \text{ cm}^{-3}$  range to produce only a single component] is responsible for the longer  $\tau_{\text{ave}}$  in the HT and Li-indiffused MG samples.

It should be noted that the above-mentioned limit of  $(2-3) \times 10^{17} \text{ cm}^{-3}$  is, in fact, not the limit for saturation trapping [which occurs at  $(2-3) \times 10^{18} \text{ cm}^{-3}$ ]. The lifetime

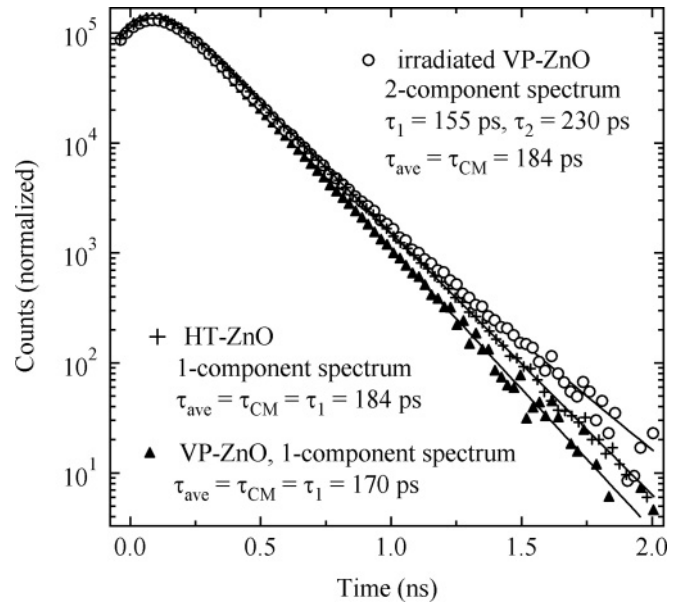


FIG. 2. Positron lifetime spectra measured for an electron-irradiated VP-ZnO sample,<sup>27</sup> a typical spectrum for HT-ZnO (as well as for Li-enriched MG-ZnO samples) and the bulk lifetime spectrum as measured in the VP-ZnO reference sample.

data recorded in samples HT-3 and HT-4 could not be separated into two components in spite of  $\tau_{\text{ave}}$  being above  $\tau_B$  by 8–9 ps, which should be enough for reliable separation when only  $V_{\text{Zn}}$  are trapping positrons. The temperature-dependent data on similar samples in Ref. 44 imply that shallow traps for positrons (e.g., negatively charged non-open volume defects such as impurities) are also present in the samples and are able to trap positrons at room temperature. Even a relatively low concentration of such defects will produce a low-intensity lifetime component equivalent to  $\tau_B$  in the decay spectra, making the separation of lifetime components in practice impossible. Hence the lower limit given for the Li-related defect concentration is an estimate of minimum concentration for the observation of a major effect in the lifetime data. Here, it should also be pointed out that residual hydrogen impurities and their formation of complexes with open volume defects, such as  $V_{\text{Zn}}$ , can play a role, as discussed in Ref. 25.

Doppler broadening experiments were performed on the samples to determine the *S*- and *W*-parameters that are specific to different annihilation states. Figure 3 shows the *W*-parameter versus the *S*-parameter for the samples HT-1, HT-2, and MG-2. The parameter values are normalized to those of positrons annihilating in the delocalized state in the ZnO crystal<sup>18</sup> and values for Zn-vacancy saturation trapping are taken from previous experiments on irradiation-induced defects in ZnO.<sup>18,21,27</sup> In Fig. 3, these points are denoted by “ZnO lattice” and “ $V_{\text{Zn}}$ ”, respectively, and the line connecting them is referred to as the  $V_{\text{Zn}}$ -line.

In samples, where the  $V_{\text{Zn}}$  is a dominant open volume positron trap, the *S*/*W* parameter values follow the  $V_{\text{Zn}}$ -line, with the experimental points gathered on a position determined by the actual  $V_{\text{Zn}}$ -concentration;<sup>18</sup> this holds for sample HT-2, where the  $V_{\text{Zn}}$  concentration can be estimated as  $5 \pm 1 \times 10^{16} \text{ cm}^{-3}$  (corresponding to *S* = 1.012 and

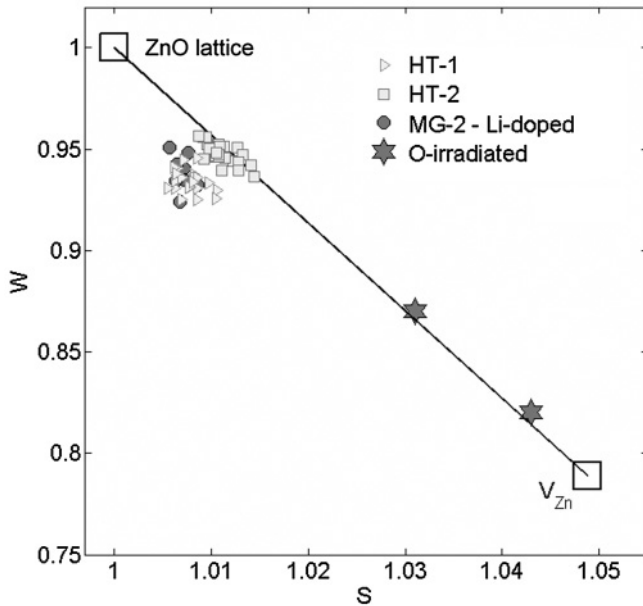


FIG. 3.  $W$ -parameter versus  $S$ -parameter as measured in the Li-rich (HT-1 and MG-2) and the Li-lean (HT-2) samples. The data points related to surface annihilation are removed for clarity. In addition, values obtained from a ZnO sample irradiated with oxygen ions, containing two different concentrations of  $V_{Zn}$ , are shown for comparison (Ref. 27).

$W = 0.947$ ), which is 1 order of magnitude higher than the total Li-concentration in the sample, see Fig. 1. Such a  $V_{Zn}$ -concentration is consistent with the average positron lifetime of 178–179 ps found after Li-removal (HT-3 and HT-4), assuming that the longer lifetime, as compared to  $\tau_B$ , is due to  $V_{Zn}$ . However, in all the measured samples containing significant amounts of Li (e.g., HT-1 and MG-2), the  $S/W$  parameter values fall below the  $V_{Zn}$ -line indicating the presence of a positron trap different from the  $V_{Zn}$ , in agreement with the lifetime results. It should be noted that in absolute numbers, the Doppler broadening results vary slightly between different HT wafers (not shown), probably due to differences in the concentration of  $V_{Zn}$  and  $Li_{Zn}$ , but all of them exhibit the same trend, where the data points fall below the  $V_{Zn}$ -line. This trend is also present for the data in Ref. 45.

In order to shed more light on the identity of the defects dominating the trapping of positrons in Li-rich samples, coincidence Doppler broadening measurements were undertaken. The so-called ratio curves, i.e., the Doppler broadening spectra measured for the HT- and in-diffused MG-samples divided by the spectrum measured for the VP reference sample, are shown in Fig. 4 together with the corresponding ratio curves obtained theoretically for the  $V_{Zn}$ , the substitutional  $Li_{Zn}$ , and the  $Li_{Zn}$ -H- $Li_{Zn}$  complex proposed in Ref. 2. Also the OH- $Li_{Zn}$  and  $Li_{Zn}$ - $Li_i$  complexes have been calculated, using the ground state configurations predicted by Wardle *et al.*,<sup>5</sup> but they are omitted in Fig. 4; the  $Li_{Zn}$ - $Li_i$  pair is not found to be active as positron trap while the curve for OH- $Li_{Zn}$  is indistinguishable from the one for  $Li_{Zn}$ . The latter result is perhaps somewhat surprising since an extra H is expected to increase the high-momentum intensity, but this is compensated by a decrease caused by outward relaxation of Li (Ref. 5)

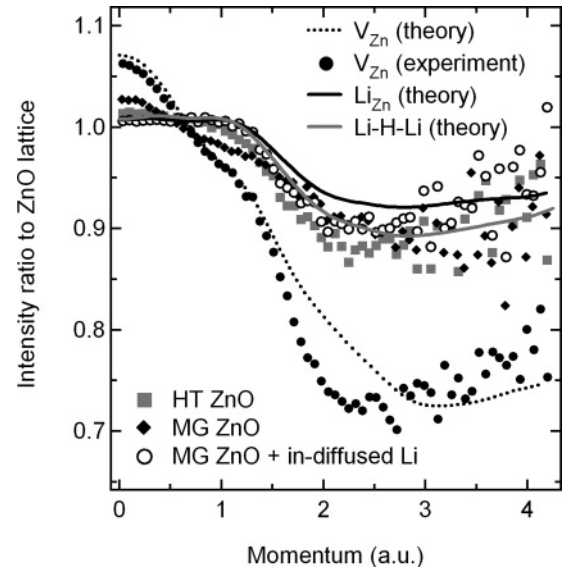


FIG. 4. Coincidence Doppler broadening measurements for as-grown HT-ZnO (HT-1), as-grown MG-ZnO, and Li-doped MG-ZnO as compared to the theoretical values obtained for  $V_{Zn}$ ,  $Li_{Zn}$ , and the  $Li_{Zn}$ -H- $Li_{Zn}$  complex. The experimental data obtained for a ZnO sample irradiated with oxygen ions with high concentration of  $V_{Zn}$  is shown for comparison (Ref. 27).

For comparison, Fig. 4 also includes data obtained for an oxygen ion-irradiated sample with a high concentration of  $V_{Zn}$ s (Ref. 27) illustrating that the features of the experimental and theoretical ratio curves (such as the shoulder at 1–1.2 a.u.) agree very well. From this, it is evident that the experimental ratio curves obtained in the Li-rich materials cannot be explained by assuming nonsaturated trapping by  $V_{Zn}$ . On the other hand, the theoretical curves for the  $Li_{Zn}$ ,  $Li_{Zn}$ -H- $Li_{Zn}$ , and OH- $Li_{Zn}$  complexes all show an excellent agreement with the data obtained from the Li-indiffused MG sample. This also holds for the lifetime measurements, where the calculated lifetime of the positron trapped at the  $Li_{Zn}$  defect is 6–8 ps longer than the bulk one depending on whether we consider the center or off-center geometries predicted by Lany and Zunger.<sup>46</sup> For the Li-H-Li defect, it is 8 ps; for OH- $Li_{Zn}$ , 7 ps; and for  $V_{Zn}$ , 81 ps longer.

It should be mentioned that our calculations predicted a bulk ZnO lifetime of 137 ps, which is considerably shorter than the experimental value of 170 ps. Such an underestimation is typical<sup>34</sup> for our specific choice of LDA parametrization<sup>38</sup> for electron-positron correlation effects, and it occurs especially for materials containing electronic states derived from atomic  $d$  orbitals. We stress that we have chosen the approximations we use so that the Doppler ratio spectra, rather than the positron lifetimes, would be reproduced in accordance with experiments as well as possible (please see the benchmarks done for other materials in Ref. 34). However, even though the absolute values of the positron lifetimes do not match, lifetime differences between the defect lifetimes and the bulk lifetime give a valid comparison between experiments and theory.

As will be discussed below, the concentration of the dominant positron trap in the Li-indiffused MG sample is at least  $(2-3) \times 10^{18} \text{ cm}^{-3}$ , which exceeds the hydrogen content of  $\leq 6 \times 10^{17} \text{ cm}^{-3}$  in the sample, as determined by SIMS and

limited by the sensitivity of the measurements, by a factor of 5 (or more). Thus, it can be concluded that the main positron trap is  $\text{Li}_{\text{Zn}}$ , with only a minor contribution (if any) from  $\text{Li}_{\text{Zn}}\text{-H-Li}_{\text{Zn}}$  and  $\text{OH-Li}_{\text{Zn}}$ . The low H concentration also excludes the  $\text{V}_{\text{Zn}}\text{-H}_n$  complexes suggested by Brauer *et al.*<sup>25</sup>

The differences between the  $\text{V}_{\text{Zn}}$  and  $\text{Li}_{\text{Zn}}$  ratio spectra in Fig. 4 are largely explained by the smaller open volume seen by the positron in the latter case. The Li repels the positron toward neighboring ion cores thereby increasing the high-momentum intensity relative to the  $\text{V}_{\text{Zn}}$  spectrum. The direct contribution of the Li orbitals to the  $\text{Li}_{\text{Zn}}$  spectrum can be quantified by considering the system as a superposition of free atoms and decomposing the total annihilation rate to contributions due to different atomic orbitals. The Li contribution turns out to be only 5% of the total annihilation rate. Furthermore, the direct Li contribution to the Doppler spectrum is rather featureless. In conclusion, our calculations indicate that we do not observe any clear “Li fingerprint”, which would provide the possibility to unambiguously identify Li-related defects in a more general case. However, the flat region with the ratio slightly above 1.0 extending from 0 to 1.3 a.u. is unique for  $\text{Li}_{\text{Zn}}$ . It has been found previously<sup>42</sup> in the GaN-system that addition of hydrogen to vacancy defects flattens out the ratio curves slightly, but preserves the qualitative features (such as the shoulder observed between 1 and 1.2 a.u.).

The data in Fig. 4 obtained for HT ZnO also match closely to  $\text{Li}_{\text{Zn}}$  but a small contribution from  $\text{V}_{\text{Zn}}$  (without Li) can be revealed (namely, the slightly higher intensity at low momenta, and a hint of a shoulder-like feature at around 1 a.u.). According to Sann *et al.*,<sup>2</sup> the  $\text{Li}_{\text{Zn}}\text{-H-Li}_{\text{Zn}}$  complex does not appear in as-grown HT-material and it has also been found previously that the concentration of  $\text{OH-Li}_{\text{Zn}}$  is low compared to the total concentration of Li in as grown HT ZnO.<sup>10</sup> Hence,  $\text{Li}_{\text{Zn}}$  occurs as the dominant trap also in HT ZnO, but with detectable contribution from  $\text{V}_{\text{Zn}}$ . In the as-received MG sample, the high-momentum (above 1.5 a.u.) region displays similar intensity as that in the HT sample while in the low-momentum region (less than 0.5 a.u.), the MG sample exhibits clearly higher intensity, consistent with nonsaturation trapping by  $\text{V}_{\text{Zn}}$ . Thus, these data give clear evidence of the presence of  $\text{V}_{\text{Zn}}$  in the near surface region of the as-received MG sample, even if the lifetime experiments employing fast positrons show a  $\text{V}_{\text{Zn}}$  concentration below the detection limit in the bulk of the sample. This is not surprising as surface treatments are known to affect the ZnO crystal on the scale of several microns below the surface.<sup>32</sup>

When positrons are trapped by one type of defect, saturation trapping is observed in lifetime experiments when the trapping rate at a given defect is  $\kappa_d = \tau_B^{-1} (\tau_{\text{ave}} - \tau_B) / (\tau_d - \tau_{\text{ave}}) \gtrsim 20 \tau_B^{-1}$ , where  $\tau_d$  is the defect positron lifetime. Using the typical value for the trapping coefficient for negatively charged defects,  $\mu_d = 3 \times 10^{15} \text{ s}^{-1}$  (Ref. 18), a defect concentration of about  $(2\text{-}3) \times 10^{18} \text{ cm}^{-3}$  is required for saturation trapping. However, if several kinds of defects (with comparable concentration) compete in positron trapping, a lower concentration (of roughly 1 order of magnitude) is sufficient for producing a lifetime spectrum where the components of the different defects cannot be resolved. In this case, it is primarily the lifetime of the dominant defect species that defines the

lifetime spectrum. The latter situation is encountered for the HT-1 sample (as-grown) where, in addition to  $\text{Li}_{\text{Zn}}$ , a detectable concentration of  $\text{V}_{\text{Zn}}$  is present as well. In order to produce data resembling saturation trapping, as observed in Fig. 2, essentially all of the Li atoms in sample HT-1 ( $2 \times 10^{17} \text{ cm}^{-3}$ ) must reside on the Zn-site, in accordance with previously reported results for electrical measurements of similar samples.<sup>11,12</sup> The  $\text{V}_{\text{Zn}}$  concentration in sample HT-1 is difficult to determine with a high degree of accuracy, but an approximate value of  $5 \times 10^{16} \text{ cm}^{-3}$  can also be deduced taking into account the results in Fig. 4. Interestingly, from the Doppler broadening data (Fig. 3), a similar value of the  $\text{V}_{\text{Zn}}$  concentration is obtained for sample HT-2 (post-growth annealed and Li-lean). In this sample,  $\text{V}_{\text{Zn}}$  is the prevailing positron trap, and these data may suggest that the content of  $\text{V}_{\text{Zn}}$  already exists after growth and remains during the high temperature postgrowth treatment. However, we would like to point out that the isolated  $\text{V}_{\text{Zn}}$  has previously been found to anneal out already at 300 °C.<sup>21</sup> Thus, the  $\text{V}_{\text{Zn}}$  observed in the as-grown and thermally treated ZnO crystals may not be in its isolated form, but rather be stabilized by other intrinsic defects or impurities (including hydrogen). However, since they retain their  $\text{V}_{\text{Zn}}$ -like defect characteristics from the PAS point of view even when complexed with substitutional impurities, they are labeled  $\text{V}_{\text{Zn}}$  for simplicity. In principle, also  $\text{Li}_{\text{Zn}}$  could be regarded as a  $\text{V}_{\text{Zn}}$  perturbed by a Li-atom inside the open volume, but the clearly different Doppler broadening signal (e.g., no shoulder at 1–1.2 a.u.) justifies the use of  $\text{Li}_{\text{Zn}}$ .

For the Li-indiffused MG-2 sample containing  $1.5 \times 10^{19} \text{ Li/cm}^3$ , there is no detectable contribution from  $\text{V}_{\text{Zn}}$  (Figs. 3 and 4) and  $\text{Li}_{\text{Zn}}$  leads to saturation trapping on its own, i.e., the difference in the positron lifetime of 10 ps relative to the VP reference sample occurs without the presence of the clearly longer lifetime component of  $\text{V}_{\text{Zn}}$  illustrated for the electron-irradiated sample in Fig. 2. Thus, at least  $(2\text{-}3) \times 10^{18} \text{ cm}^{-3}$  of the Li-atoms must exist as  $\text{Li}_{\text{Zn}}$ , but no p-type conductivity was detected. If an acceptor state located 0.26 eV above the valence band edge ( $E_v$ ) (Ref. 3) for  $\text{Li}_{\text{Zn}}$  together with ordinary thermal ionization is assumed, this would yield a hole concentration of  $\geq 10^{16} \text{ cm}^{-3}$  at room temperature. However, the sample is highly resistive ( $>10 \text{ k}\Omega \text{ cm}$ ) indicating that self-compensation, presumably caused by  $\text{Li}_i$ , prevails at high Li-concentrations. Alternatively, formation of electrically inactive  $\text{Li}_{\text{Zn}}\text{-Li}_i$  pairs may be pronounced in highly doped materials, as suggested by Wardle *et al.*,<sup>5</sup> but this does not account for the nondetectable hole concentration in the in-diffused MG-2 sample unless the acceptor state of  $\text{Li}_{\text{Zn}}$  is substantially deeper than 0.26 eV above  $E_v$  or a balancing donor concentration exists.

Finally, it should be noted that the positron data do not provide evidence on the exact position of Li on the substitutional Zn-site. We performed *ab initio* calculations for both the negatively charged on-center and the neutral off-center configurations predicted by Lany *et al.*,<sup>46</sup> and, interestingly,<sup>47</sup> found negligible differences in predicted positron localization, lifetime, and Doppler broadening signals. A convergence test was performed using a larger 768-atom supercell, which is unfortunately currently too large to allow accurate calculations of Doppler spectra; we observe no significant difference in

the localized positron density between the 96- and 768-atom supercells and find that the calculated positron lifetimes agree within 2 ps. Using the 768-atom cell, we estimate the positron binding energies to the Li-related defects examined to be on the order of 0.2–0.3 eV. Similar calculations made for semiconductor point defects, in general, underbind the positron,<sup>48</sup> so we regard this estimate as a lower bound for the binding energy and do not expect positron detrapping from defects to play a role in measurements. For  $V_{\text{Zn}}$ , a much deeper positron trap, we estimate the positron binding energy to be on the order of 2 eV.

#### IV. CONCLUSION

In conclusion, the positron annihilation signature of negatively charged substitutional Li,  $\text{Li}_{\text{Zn}}$ , has been identified. It has an open volume smaller than that of the  $V_{\text{Zn}}$ . Essentially, all Li atoms present in n-type HT ZnO reside on the Zn-site and the resulting open volume is thus responsible for the

increase in the single-component positron lifetime observed in as-grown HT ZnO as compared to samples produced by other growth techniques yielding Li-lean material. This also explains the discrepancy in the reported values for the bulk positron lifetime in ZnO, but further work still remains to fully elucidate the role of residual hydrogen impurities and their interaction with intrinsic open volume defects. A large concentration of  $\text{Li}_{\text{Zn}}^- (\geq 10^{18} \text{ cm}^{-3})$  is observed after in-diffusion of Li at 600 °C, but no p-type conductivity is detected indicating that self-compensation prevails in highly doped samples with a total Li concentration in excess of  $10^{19} \text{ cm}^{-3}$ .

#### ACKNOWLEDGMENTS

Financial support from the FUNMAT@UiO-program and the Norwegian Research Council (NANOMAT and FRINAT programs), NORDFORSK and the Academy of Finland is gratefully acknowledged.

- 
- <sup>1</sup>R. T. Cox, D. Block, A. Hervé, R. Picard, C. Santier, and R. Helbig, *Solid State Commun.* **25**, 77 (1978).
- <sup>2</sup>J. Sann, A. Hofstaetter, D. Pfisterer, J. Stehr, and B. K. Meyer, *Phys. Status Solidi C* **3**, 952 (2006).
- <sup>3</sup>O. Lopatiuk, L. Chernyak, A. Osinsky, and J. Q. Xie, *Appl. Phys. Lett.* **87**, 214110 (2005).
- <sup>4</sup>J. J. Lander, *J. Phys. Chem. Solids* **15**, 324 (1960).
- <sup>5</sup>M. G. Wardle, J. P. Goss, and P. R. Briddon, *Phys. Rev. B* **71**, 155205 (2005).
- <sup>6</sup>A. Carvalho, A. Alkauskas, A. Pasquarello, A. Tagantsev, and N. Setter, *Physica B* **404**, 4797 (2009).
- <sup>7</sup>L. E. Halliburton, L. Wang, L. Bai, N. Y. Garces, N. C. Giles, M. J. Callahan, and B. Wang, *J. Appl. Phys.* **96**, 7168 (2004).
- <sup>8</sup>E. V. Lavrov, *Physica B* **340-342**, 195 (2003).
- <sup>9</sup>G. A. Shi, M. Stavola, and W. B. Fowler, *Phys. Rev. B* **73**, 081201 (2006).
- <sup>10</sup>K. M. Johansen, H. Haug, Ø. Prytz, P. T. Neuvonen, K. E. Knutsen, L. Vines, E. V. Monakhov, A. Y. Kuznetsov, and B. G. Svensson, *J. Electron. Mater.* **40**, 429 (2011).
- <sup>11</sup>B. G. Svensson, T. M. Børseth, K. M. Johansen, T. Maqsood, R. Schifano, U. Grossner, J. S. Christensen, L. Vines, P. Klason, Q. X. Zhao *et al.*, *Mater. Res. Soc. Symp. Proc.* **1035**, L04–01 (2008).
- <sup>12</sup>L. Vines, E. V. Monakhov, R. Schifano, W. Mtangi, F. D. Auret, and B. G. Svensson, *J. Appl. Phys.* **107**, 103707 (2010).
- <sup>13</sup>P. H. Kasai, *Phys. Rev.* **130**, 989 (1963).
- <sup>14</sup>Y. J. Zeng, Z. Z. Ye, W. Z. Xu, D. Y. Li, J. G. Lu, L. P. Zhu, and B. H. Zhao, *Appl. Phys. Lett.* **88**, 062107 (2006).
- <sup>15</sup>Y. J. Zeng, Z. Z. Ye, J. G. Lu, W. Z. Xu, L. P. Zhu, B. H. Zhao, and S. Limpijumnong, *Appl. Phys. Lett.* **89**, 042106 (2006).
- <sup>16</sup>B. Meyer, J. Sann, and A. Zeuner, *Superlattices Microstruct.* **38**, 344 (2005), e-MRS 2005 Symposium G:ZnO and Related Materials – Part 1.
- <sup>17</sup>S. Brunner, W. Puff, A. G. Balogh, and P. Mascher, *Mater. Sci. Forum* **363-365**, 141 (2001).
- <sup>18</sup>F. Tuomisto, V. Ranki, K. Saarinen, and D. C. Look, *Phys. Rev. Lett.* **91**, 205502 (2003).
- <sup>19</sup>Z. Chen, M. Maekawa, and A. Kawasuso, *Chin. Phys. Lett.* **23**, 675 (2006).
- <sup>20</sup>R. M. de la Cruz, R. Pareja, R. González, L. A. Boatner, and Y. Chen, *Phys. Rev. B* **45**, 6581 (1992).
- <sup>21</sup>F. Tuomisto, K. Saarinen, D. C. Look, and G. C. Farlow, *Phys. Rev. B* **72**, 085206 (2005).
- <sup>22</sup>Z. Q. Chen, S. Yamamoto, M. Maekawa, A. Kawasuso, X. L. Yuan, and T. Sekiguchi, *J. Appl. Phys.* **94**, 4807 (2003).
- <sup>23</sup>Z. Q. Chen, A. Kawasuso, Y. Xu, H. Naramoto, X. L. Yuan, T. Sekiguchi, R. Suzuki, and T. Ohdaira, *Phys. Rev. B* **71**, 115213 (2005).
- <sup>24</sup>Z. Q. Chen, K. Betsuyaku, and A. Kawasuso, *Phys. Rev. B* **77**, 113204 (2008).
- <sup>25</sup>G. Brauer, W. Anwand, D. Grambole, J. Grenzer, W. Skorupa, J. Čížek, J. Kuriplach, I. Procházka, C. Ling, C. So *et al.*, *Phys. Rev. B* **79**, 115212 (2009).
- <sup>26</sup>T. M. Børseth, F. Tuomisto, J. S. Christensen, E. V. Monakhov, B. G. Svensson, and A. Y. Kuznetsov, *Phys. Rev. B* **77**, 045204 (2008).
- <sup>27</sup>A. Zubiaga, F. Tuomisto, V. A. Coleman, H. H. Tan, C. Jagadish, K. Koike, S. Sasa, M. Inoue, and M. Yano, *Phys. Rev. B* **78**, 035125 (2008).
- <sup>28</sup>A. Zubiaga, F. Tuomisto, F. Plazaola, K. Saarinen, J. A. Garcia, J. F. Rommeluere, J. Zuniga-Perez, and V. Munoz-Sanjose, *Appl. Phys. Lett.* **86**, 042103 (2005).
- <sup>29</sup>N. Ohashi, T. Ishigaki, N. Okada, H. Taguchi, I. Sakaguchi, S. Hishita, T. Sekiguchi, and H. Haneda, *J. Appl. Phys.* **93**, 6386 (2003).
- <sup>30</sup>N. H. Nickel and K. Brendel, *Phys. Rev. B* **68**, 193303 (2003).
- <sup>31</sup>D. G. Thomas and J. J. Lander, *J. Chem. Phys.* **25**, 1136 (1956).
- <sup>32</sup>F. A. Selim, M. H. Weber, D. Solodovnikov, and K. G. Lynn, *Phys. Rev. Lett.* **99**, 085502 (2007).
- <sup>33</sup>K. Saarinen, P. Hautojärvi, and C. Corbel, in *Identification of Defects in Semiconductors*, edited by M. Stavola (Elsevier, New York, 1998), Vol. 51, Part 1, pp. 209–285.
- <sup>34</sup>I. Makkonen, M. Hakala, and M. J. Puska, *Phys. Rev. B* **73**, 035103 (2006).

- <sup>35</sup>P. E. Blöchl, *Phys. Rev. B* **50**, 17953 (1994).
- <sup>36</sup>G. Kresse and J. Furthmüller, *Phys. Rev. B* **54**, 11169 (1996).
- <sup>37</sup>G. Kresse and D. Joubert, *Phys. Rev. B* **59**, 1758 (1999).
- <sup>38</sup>E. Boroński and R. M. Nieminen, *Phys. Rev. B* **34**, 3820 (1986).
- <sup>39</sup>M. Alatalo, B. Barbiellini, M. Hakala, H. Kauppinen, T. Korhonen, M. J. Puska, K. Saarinen, P. Hautojärvi, and R. M. Nieminen, *Phys. Rev. B* **54**, 2397 (1996).
- <sup>40</sup>I. Makkonen, M. Hakala, and M. Puska, *J. Phys. Chem. Solids* **66**, 1128 (2005).
- <sup>41</sup>M. Rummukainen, I. Makkonen, V. Ranki, M. J. Puska, K. Saarinen, and H.-J. L. Gossmann, *Phys. Rev. Lett.* **94**, 165501 (2005).
- <sup>42</sup>S. Hautakangas, I. Makkonen, V. Ranki, M. J. Puska, K. Saarinen, X. Xu, and D. C. Look, *Phys. Rev. B* **73**, 193301 (2006).
- <sup>43</sup>I. Makkonen, A. Snicker, M. J. Puska, J.-M. Mäki, and F. Tuomisto, *Phys. Rev. B* **82**, 041307 (2010).
- <sup>44</sup>F. Tuomisto and D. C. Look, in *Proceedings of SPIE*, edited by F. H. Teherani and C. W. Litton (San Jose, CA, USA, 2007), Vol. 6474, p. 647413.
- <sup>45</sup>T. M. Børseth, F. Tuomisto, J. S. Christensen, W. Skorupa, E. V. Monakhov, B. G. Svensson, and A. Yu. Kuznetsov, *Phys. Rev. B* **74**, 161202 (2006).
- <sup>46</sup>S. Lany and A. Zunger, *Phys. Rev. B* **80**, 085202 (2009).
- <sup>47</sup>It is generally thought that positron localization in a deep state requires at least a monovacancy-sized open volume. Our results suggest that the observed trapping could be possible also in other cases where the  $Z$  of the substitutional atom is much smaller than that of the host atom.
- <sup>48</sup>I. Makkonen and M. J. Puska, *Phys. Rev. B* **76**, 054119 (2007).